Could the "Janus-like" Properties of the Halobenzene CX Bond (X=Cl, Br) Be Leveraged to Enhance Molecular Recognition?

ARTICLE *in* JOURNAL OF COMPUTATIONAL CHEMISTRY · FEBRUARY 2015

Impact Factor: 3.59 · DOI: 10.1002/jcc.23786

5 AUTHORS, INCLUDING:

Krystel El Hage
University of Basel
7 PUBLICATIONS **15** CITATIONS
SEE PROFILE

Jean-Philip Piquemal
Pierre and Marie Curie University - Paris 6
111 PUBLICATIONS **2,283** CITATIONS
SEE PROFILE

Zeina Hobaika
Saint Joseph University, Lebanon
21 PUBLICATIONS **53** CITATIONS
SEE PROFILE

Richard G. Maroun
Saint Joseph University, Lebanon
76 PUBLICATIONS **492** CITATIONS
SEE PROFILE

Could the "Janus-like" Properties of the Halobenzene CX Bond (X=Cl, Br) Be Leveraged to Enhance Molecular Recognition?

Krystel El Hage,[a,b] Jean-Philip Piquemal,[c] Zeina Hobaika,[b] Richard G. Maroun,[b] and Nohad Gresh*[a]

The CX bond in halobenzenes (X=Cl, Br) exhibits a dual character, being electron-deficient along the CX direction, and electron-rich on its flanks. We sought to amplify both features by resorting to electron-withdrawing and electron-donating substituents, respectively. This was done by quantum chemistry (QC) computations in the recognition sites of three protein targets: farnesyl transferase, coagulation factor Xa, and the HIV-1 integrase. In this context, some substituents, notably fluorine, CF_3, and $NHCH_3$, afforded significant overall gains in the binding energies as compared to the parent halobenzene, in the 2–5 kcal/mol range. In fact, we found that some di- and up to tetra-substitutions enabled even larger gains than those they contribute separately owing to many-body effects. Moreover, desolvation was also found to be a key contributor to the energy balances. As a consequence, some particular substituents, contributing to reduce the halobenzene dipole moment, accordingly reduced solvation: this factor acted in synergy with their enhancement of the intermolecular interaction energies along and around the CX bond. We could thus leverage the "Janus-like" properties of such a bond and the fact that it can be tuned and possibly amplified by well-chosen substituents. We propose a simple yet rigorous computational strategy resorting to QC to prescreen novel substituted halobenzenes. The QC results on the recognition sites then set benchmarks to validate polarizable molecular mechanics/dynamics approaches used to handle the entirety of the inhibitor-protein complex. © 2014 Wiley Periodicals, Inc.

DOI: 10.1002/jcc.23786

Introduction

An outstanding property of Cl, Br, and I halobenzenes is the presence of a zone of electron depletion prolonging the C—X bond, denoted as the "sigma-hole," coexisting with a zone of electron build-up on the sides of this bond.[1] The first feature has focused significant interest,[2] and numerous examples showed the CX bond pointing directly either toward an electron-rich atomic site or toward the center of the electron-rich aromatic rings. Examples are provided by protein[3–10] and DNA[11] recognition sites of halobenzenes, and by molecular crystals.[12] Except for a few recent examples, conversely,[13] the second feature has so far attracted a much lesser attention. This has motivated us to try and leverage the double-faceted, "Janus-like," nature of halobenzenes to optimize their affinities for targeted sites, by: (a) increasing electron-depletion along the CX bond by electron-withdrawing substituents and (b) conversely, enhancing electron density on the sides of this bond by electron-donating substituents. The impact of both kinds of substitutions are quantified by intermolecular interaction (ΔE) calculations in the binding site of three proteins, and are performed using dispersion-corrected DFT.

We consider three protein halobenzene binding sites recently unraveled by high-resolution X-ray diffraction. These are farnesyl transferase (Ftase),[14] coagulation FXa (factor Xa),[15] and the HIV-1 integrase (INT).[16] Such structures show that the halobenzene can reside in the neighborhood of electron-rich as well as of electron-deficient sites of the receptor. Its binding to either kind of site could therefore be enhanced by well-defined substituents respectively deplenishing or replenishing the CX electron density. The impact of such substitutions is quantified by DFT-d ΔE computations. We further investigate the possibility for selected electron-donating and electron-attracting substituents to coexist within the same halobenzene molecule and amplify in concert each facet of the "Janus-like" CX bond, thus favorably impacting ΔE. The electrostatic effects of such substitutions on both regions of the sigma-hole are analyzed by mapping the molecular electrostatic potential (MEP) of the halobenzenes. Furthermore, some substituents, on reducing the halobenzene molecular dipole, could accordingly reduce its desolvation energy. This factor would then act in synergy with the ΔE enhancement in the energy balances.

[a] *K. El Hage, N. Gresh*
Chemistry and Biology, Nucleo(s)tides and Immunology for Therapy (CBNIT), UMR 8601 CNRS, UFR Biomédicale, Paris, France
E-mail: nohad.gresh@parisdescartes.fr
[b] *K. El Hage, Z. Hobaika, R. G. Maroun*
Centre d'Analyses et de Recherche, UR EGFEM, LSIM, Faculté des Sciences, Saint Joseph University of Beirut, B.P. 11-514 Riad El Solh, Beirut, 1107 2050, Lebanon
[c] *J-P. Piquemal*
Laboratoire de Chimie Théorique, Sorbonne Universités, UPMC, UMR7616 CNRS, Paris, France

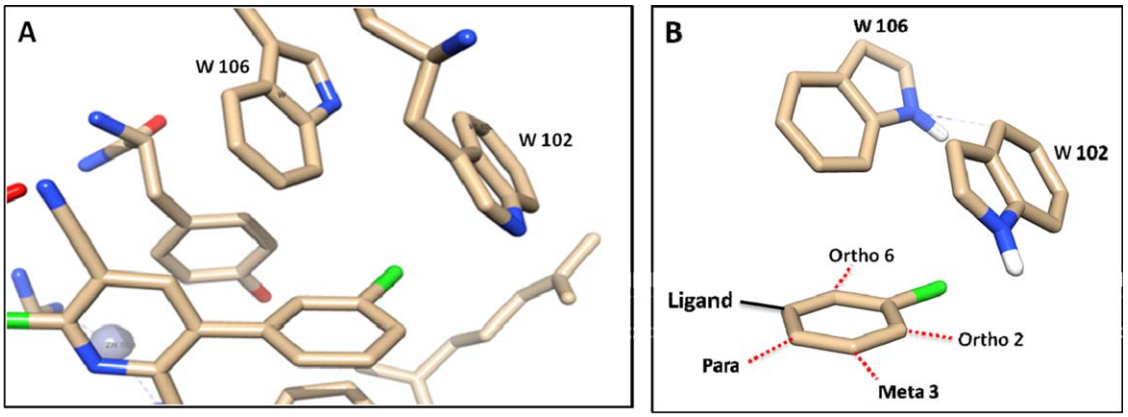

Figure 1. a) Representation of the binding site of Ftase; and b) close-up on the interaction involving the halobenzene ring and notation of the substitution positions.

Methods

All intermolecular interaction energies were computed by quantum chemistry (QC) at the correlated level, using the dispersion-corrected B97-d functional by Grimme .[17] We used the aug-cc-pVTZ(-f) basis set.[18] Energy-minimization was done using the Berny procedure[19] and the G09 software.[20] The values of ΔE were corrected for the basis set superposition error.[21] The solvation energies of the uncomplexed halobenzenes were computed with the C-polarizable continuum model (PCM) procedure, a Conductor-like polarizable continuum model.[22]

The complex within the recognition site was not solvated, as it is buried in the protein binding site. The binding energy $\Delta E_{binding}$ is expressed as:

$$\Delta E_{binding} = \Delta E_{complex} - (E_{prot/DNA} + E_{lig}) \quad (1)$$

It represents the difference between the energy of the complex and those of the individual interacting molecules. $\Delta E_{complex}$ is the energy of the complex after optimization. $E_{prot/DNA}$ is the energy of the protein or DNA binding site. E_{lig} is the energy of the ligand optimized prior to interaction in a water continuum.

The energy balances are completed on including the desolvation energy of the inhibitor, $\delta\Delta G_{solv}$ prior to binding, so that $\Delta E_{fin} = \Delta E_{binding} + \delta\Delta G_{solv}$. ΔE_{fin} is thus the final energy balance.

We have in addition computed the contribution of vibrational, rotational and translational entropies to correct ΔE and approach the free energies (ΔG). This was done using the G09 thermodynamical analysis module.[20,23]

The MEPs used the electron density from the Gaussian calculations and were obtained by Gaussview5[23] for mapping. We will denote by $\alpha+$ and $\alpha-$ the zones of electron depletion and of electron build-up, respectively. For representative halobenzene derivatives, analyses of the electron populations and volumes on the halogen atom were done using the electron localization function (ELF) analysis.[24]

Other DFT functionals could be used concurrently, such as M06-2X[25] or WB97x.[26] We have selected here the B97-d functional on account of its extensive testings.

We would also like to note that all QC calculations are performed, as is common usage, with a dielectric constant of one, even though they aim at reproducing interactions taking place in a protein active site. This seems amply justified since we are dealing with local interactions, and it could be problematic to anticipate how neighboring residues could modulate the "real" dielectric constant, which is a macroscopic quantity.

Following a remark made by a Reviewer, we wish to stress that for all three binding sites considered in the present study, we will probe the impact of substitutions on the affinities of the halobenzenes to the sole two receptor sites of their binding cleft. We do not attempt to take into account the impact on their affinities for other, more distant protein residues: indeed, this would only be meaningful if the entirety of the inhibitor were considered and relaxed as well, anchoring the halobenzene and preventing it to drift away from its cleft. This is not the purpose of the present approach, but is to be considered as a next stage in the context of polarizable molecular mechanics/dynamics potentials, following a validation of such potentials on model sites by the present, or related, QC computations.

Results and Discussion

Binding site of farnesyl transferase

Ftase is a Zn-metalloenzyme which activates guanosine triphosphate (GTP)-binding proteins involved in cell cycle progression by catalyzing the transfer of a fifteen-carbon isoprenoid to their C-terminal group. Overactivation of these proteins results in several pathologies, which could be prevented by Ftase inhibitors. We have considered the structure of Ftase complexed with an inhibitor built out of four aromatic rings, including one chlorobenzene, seen in the X-ray structure (PDB 1NI1)[14] to bind to two tryptophan rings, W102 and W106. This structure is represented in Figure 1a, and a close-up together with the available substitution positions is shown in Figure 1b. In all that follows, the substitution positions (ortho, meta or para) will be denoted with respect to the Cl atom. The same notations will be used with the two other target enzymes. We considered a ternary complex formed by the halobenzene derivative and the end side-chains of W102 and

Table 1. Binding site of farnesyl transferase.

		W106 - halobenzyl			W102-halobenzyl		Ternary complex	
Complex A		$\delta\Delta G$Solv	ΔE Gas	ΔE Gas - $\delta\Delta G$Solv	ΔE Gas	ΔE Gas - $\delta\Delta G$Solv	ΔE Gas	ΔE Gas - $\delta\Delta G$Solv
Para	NH_2	−5.98	2.35	8.3	−3.64 $\uparrow\alpha^-$	2.34	−0.33	5.65
	OH	−7.54	3.4	10.94	−3.41 $\uparrow\alpha^-$	4.13	−0.15	7.39
	$NHCH_3$	−4.49	2.84	7.33	−4.9 $\uparrow\alpha^-$	−0.41	−1.85	2.64
	CF_3	−0.54	3.01	3.55	−4.14	−3.6	−1.27	−0.73
	F	−0.25	3.45	3.7	−2.74	−2.49	0.43	0.68
	NO_2	−3.85	2.56	6.41	−5.29	−1.44	−2.93	0.92
Meta 3	NH_2	−5.39	1.83	7.22	−4.92	0.47	−2.42	2.97
	OH	−7.43	2.64	10.07	−3.25	4.18	−0.73	6.7
	$NHCH_3$	−3.98	2.75	6.73	−3.84	0.14	−1.39	2.59
	CF3	−0.52	2.76	3.28	−4.23	−3.71	−1.49	−0.97
	F	0	2.67	2.67	−2.78	−2.78	−0.36	−0.36
	NO_2	−3.78	1.4	5.18	−4.94	−1.16	−3.67	0.11
Ortho 2	NH_2	−3.77	3.76	7.53	−5.29	−1.52	−1.03	2.74
	OH	−2.83	2.71	5.54	−3.48	−0.65	−0.63	2.2
	$NHCH_3$	−1.44	−0.19	1.25	−3.1	−1.66	−3.06	−1.62
	F	−0.33	2.91	3.24	−1.78	−1.45	0.89	1.22
	NO_2	−4.83	1.48	6.31	−5.1	−0.27	−2.82	2.01
Ortho 6	NH_2	−3.79	−4.84	−1.05	1.35 $\uparrow\alpha^-$	5.14	−3.08	0.71
	OH	−2.68	3.2	5.88	−4.25	−1.57	−0.95	1.73
	$NHCH_3$	−1.5	−3.5	−2	0.73	2.23	−3.01	−1.51
	F	−0.34	1.37	1.71	−0.47	−0.13	0.74	1.08
	NO_2	−4.83	−6.36	−1.53	0.82 $\uparrow\alpha^-$	5.65	−4.09	0.74
4F—m3—p—o2—o6		0.81	2.65	1.84	−4.92	−5.73	−2.28	−3.09
NHCH3—o6 CF3—m3		−2.91	−3.1	−0.19	−6.68	−3.77	−7.55	−4.64
NHCH3—o6 F—m3—p		−1.94	−1.72	0.22	−5.71	−3.77	−5.86	−3.92
CF3—m3 F—p—o2—o6		−0.15	3.29	3.44	−6.64	−6.49	−3.3	−3.15

Values (kcal/mol) of the desolvation and interaction energies and energy balances of substituted halobenzenes with respect to unsubstituted chlorobenzene

W106, namely their indole rings. The ternary complex was optimized by energy-minimizing the sole halobenzene, as W102 and W106 are considered to be held in place by the protein. The structural rearrangement of halobenzene was found to be extremely limited, and this was also the case for the substituted halobenzene. It could be noted that even without protein relaxation, some derivatives are found to have an enhanced affinity to the model binding site with respect to the parent compound (see below), so that augmented relaxation, if any, would further augment such a relative stability. We then considered five different substituents in the para, meta, ortho2, and ortho6 positions. These are three electron-donating groups, —NH_2, —OH, and —$NHCH_3$, and two electron-withdrawing ones, —CF_3 and —NO_2. The results of the energy calculations are regrouped in Table 1. The corresponding results of unsubstituted benzenes are taken as energy zeroes. For the binary complexes of each halogen with W106 and W102, and for its ternary complex, Table 1 lists: (a) the relative desolvation energy of the ligand, $\delta\Delta G$solv, given in the first column; (b) its *in vacuo* interaction energy, ΔE(gas); and (c) the partial relative energy balance, ΔE(gas)–$\delta\Delta G$solv.

Among electron-withdrawing groups, a —CF_3 in para or in meta3 appears most effective, with overall gains of −0.7 and −1.0 kcal/mol, respectively. The corresponding ΔE gains of −1.3 and −1.5 are reduced by 0.5 kcal/mol by relative desolvation with respect to the parent compound. These gains result from increased electron density depletion along the CCl bond, favoring the interaction with the electron-rich indole ring of W102. In addition, the desolvation energy undergoes a further decrease (≈0.5 kcal/mol) with respect to the parent halobenzene. No CF_3 substituent was placed in the ortho positions on account of steric repulsion with the CCl bond. Substitution by a more effective attractor, NO_2 in meta3 or in ortho2 affords significant ΔE enhancements, occurring again with W102 (−4.9 and −5.1 kcal/mol, respectively). However, these energy gains are counteracted by significantly enhanced desolvation energies in the 3.8–4.8 kcal/mol range.

Among electron donors, an —$NHCH_3$ substituent when placed in ortho2 or ortho6, afforded ΔE gains of app −1.5 kcal/mol. They stem from enhanced gas-phase interactions, ΔE (gas), occurring with W102 and W106 (resp.) and amounting to −3.5 kcal/mol. Such gains, denoted as $\delta\Delta E$ (gas), are opposed by more unfavorable 1.4–1.5 kcal/mol desolvation enthalpies compared to the parent compound. The desolvation enthalpies with —NH_2 and —OH substituents are significantly larger than for the —$NHCH_3$ derivatives, rendering the overall energy balances unfavorable whatever the substitution position.

Polysubstituted derivatives were next considered to further improve the energy balances, δE. Thus a tetra-fluoro-substituted chlorobenzene afforded a −3.1 kcal/mol δE gain, due to both ΔE (gas) and δGsolv. A similar gain (−3.2 kcal/mol) obtains if one F atom is replaced by a —CF_3 group. This derivative has a −1.7 kcal/mol more favorable ΔE(gas) with W102 opposed by a less favorable desolvation energy and more unfavorable interaction with W106. It is noteworthy that

Table 2. Comparison of ΔG_{solv} obtained by C-PCM calculations and of the experimental ΔG_{solv} values.

ΔG_{solv} (kcal/mol)	C-PCM	Experimental
benzene	−1.62	−0.86
chlorobenzene	−1.87	−1.12
1,2-dichlorobenzene	−2.03	−1.36
1,3-dichlorobenzene	−1.67	−0.98
1,4-dichlorobenzene	−1.76	−1.01

This Table is accompanied by the correlation trend.

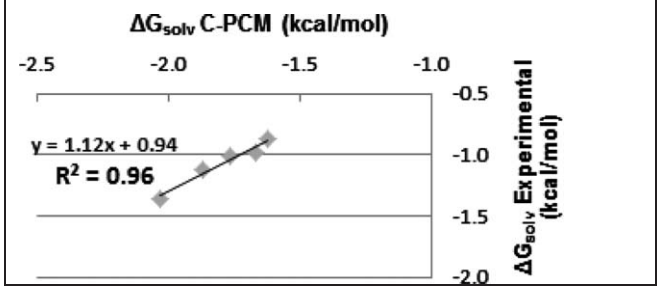

a combination of one electron-donating group, —$NHCH_3$ in ortho6, and of an electron-withdrawing group, such as a —CF_3 in meta3 or a —F in both meta3 and para, improved the energy balances by up to −4.6 and −3.9 kcal/mol (resp.). This was due to an enhancement of ΔE (gas) both with W106 due to —$NHCH_3$ as an electron donating group and with W102 due to —CF_3 or —F substituents as electron attractors. Such a simultaneous enhancement could serve to highlight the "Janus-like" property of the CCl bond of chlorobenzene.

At this stage, it could be essential to evaluate the accuracy of the ΔGsolv calculations in implicit solvent, as even small errors could impair the energy balances in the series of chlorobenzene derivatives. To address this point, we have computed the values of C-PCM ΔGsolv values for benzene, chlorobenzene, and three dichlorobenzene derivatives, for which experimental values are available.[27] The comparisons are reported in Table 2. While the C-PCM values are larger by 0.8 kcal/mol than the experimental values, the trends of ΔGsolv as a function of mono- and polysubstitution are reliably followed, with a r^2 of 0.96. This should lend credence to the energy balances which include ΔGsolv, at least within a given family of related compounds.

Binding site of coagulation factor Xa

FXa is a serine protease playing an essential role in the blood coagulation cascade which can lead to blood clotting and thrombosis. Inhibitors of FXa are endowed with anticoagulant properties and are used against thrombotic disorders. The structure of the complex of FXa with an inhibitor having a 2-carboxyindole substituent was recently solved by X-ray crystallography (PDB 2BQW).[15] This inhibitor has a chlorobenzene ring, which binds to the main-chain of G226 and to the phenol ring of Y228 (Fig. 2a). A close-up is given in Figure 2b. Accordingly, the ternary complexes considered are those of the halobenzene, the phenol ring, and a formamide fragment representing the main-chain. The results of the energy computations are reported in Table 3. Both a polar electron-donating substituent, —OH, and a polar electron-withdrawing one, —NO_2, had very unfavorable relative energy balances (δE) in the 2.3–7 kcal/mol range. This is due to highly unfavorable $\delta\Delta G$solv values, along with modest ΔE (gas) values. In marked contrast, an F substituent either in ortho2 or ortho6, afforded δE gains of −2.2 and −2.5 kcal/mol, respectively. An F substituent acts as an inductive electron-withdrawing group: it could thus enhance ΔE (gas) for the interaction of the electron-rich CO bond of Y228 with the $\alpha+$ zone of the CCl bond. It could, conversely, weaken the interaction of the electron-deficient NH bond of main-chain G226 with the $\alpha-$ zone of the CCl bond. Such a weakening is nevertheless negligible (<0.2 kcal/mol). The impact of $\delta\Delta G$solv is very small as well. Thus, for both ortho F derivatives, the gain in $\delta\Delta E$ stems from ΔE (gas). Whether in meta or in ortho, an electron-donating NH_2 substituent reinforces ΔE (gas). This is due, on the one hand, to a hydrogen bond interaction of this group with the hydroxyl oxygen of the Y228 ring (ΔE (gas) from −3.7 to −5.1 kcal/mol), but also, conversely, to the reinforcement of the interaction of the $\alpha-$ region with the G226 backbone (from −1 to −1.6 kcal/mol). These gains are counteracted by relatively large $\delta\Delta G$solv values in the 3.8 to 5.4 kcal/mol range. Except for NH_2 in meta3, the resulting δE gains in the −1.6 −2.8 kcal/mol range are comparable to those with the electron attractor fluorine in both ortho positions.

We next considered the impact of a double —F substitution. This search has focused on electron-withdrawing groups, namely two fluorines. The results on both the previous and following sections indicate that electron-donating groups could, nevertheless, also be advantageous, a possibility which, regarding this specific binding site, could certainly be left open for future studies. Thus we selected the two farthest positions from the target site, namely meta3 and meta5. This discards the possibility that the possible gains in ΔE (gas) would stem from direct interaction of fluorine with the target sites. In contrast with the situation with Ftase, the resulting $\delta\Delta E$ gain was weak (−0.3 kcal/mol). The −0.5 kcal/mol gain in ΔE (gas) with the phenol ring was accompanied by a comparable loss with the G226 main-chain. It is only because of a more favorable $\delta\Delta G$solv that a modestly favorable $\delta\Delta E$ could be recovered. We have also considered the nearest positions from the target site, ortho2 and ortho6. The resulting binding energy, with each partner and with the whole target site, was less favorable than both monosubstitutions on both positions ortho2 and ortho6.

Overall the most advantageous substitutions are either with a —F in positions ortho2 or ortho6 which further deplete the $\alpha+$ zone ($\delta\Delta E$ in the range −2.2−2.4 kcal/mol) or with an -NH_2 in positions meta5, ortho2, or ortho6 which aims to replenish the $\alpha-$ zone ($\delta\Delta E$ in the range −1.6−2.5 kcal/mol).

Binding site of HIV-1 integrase

INT is involved in the integration of viral DNA into host DNA and is the target of several efficient anti-HIV-1 drugs. The X-ray structure of the closely related foamy virus INT in its complex with a viral DNA and the drug elvitegravir was solved by high-resolution X-ray crystallography (PDB 3L2U).[16] This drug is

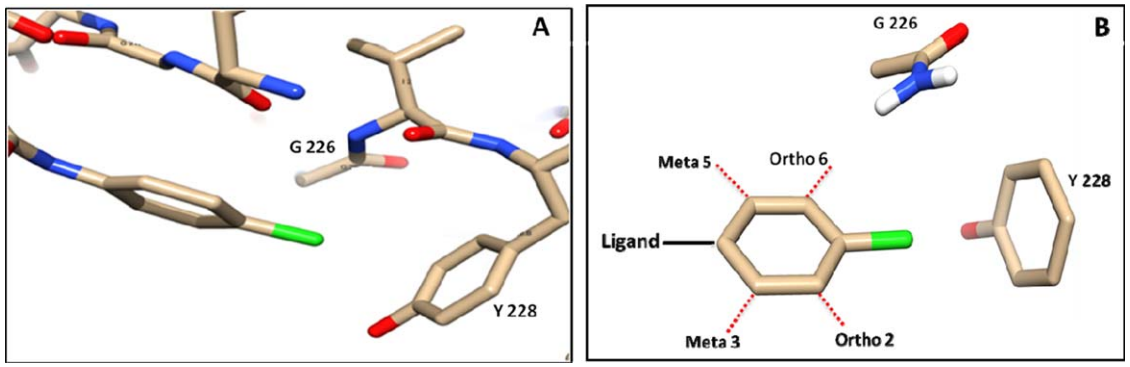

Figure 2. a) Representation of the binding site of coagulation FXa; and b) close-up on the interaction involving the halobenzene ring and notation of the substitution positions.

made out of three fragments. The central fragment is a bicyclic monoketo ring substituted with a carboxylate group. It is connected to a substituted alcoholic group (1-hydroxymethyl-2-methylpropyl) and to a 3-chloro-2-fluoro benzene ring. The X-ray structure shows that the central fragment binds to two divalent Mg(II) cations and is stacked over an adenine base, A17. The bulky alcoholic group does not interact with the protein but it is considered to effectively hinder the rotation of the adenine into a position where it stacks against the elvitegravir (EVG) metal-chelating scaffold.[28] These interactions anchor the halobenzene ring in a stacking interaction over a cytosine base, C16, while its CCl bond points toward the center of the six-membered ring of a guanine, G4 (Fig. 3). The ternary complexes thus involve the halobenzene, G4, and C16. Several substitutions were considered with the o6-fluorine removed. The energy balances with different substitutions are reported in Table 4. The energy zero is that of the complexes with the 'parent' benzene ring of elvitegravir chlorinated and fluorinated.

The double-faceted nature of the CCl bond was exemplified in two representative cases. Thus the electron-withdrawing group —F in para increased the affinity of its $\alpha+$ zone for G4 by −0.5 kcal/mol and decreased that of its $\alpha-$ zone for C16 by 0.4 kcal/mol. By contrast, the electron-donating group —OH in ortho2 group decreased the affinity of the $\alpha+$ zone for G4 by 1.2 kcal/mol and increased that of the $\alpha-$ zone for C16 by −3.2 kcal/mol.

The most efficient electron-withdrawing substitutions are with -CF_3 in para ($\delta\Delta E$ = −1.6 kcal/mol), and with -NO_2 in both ortho2 and ortho6 positions ($\delta\Delta E$=−2.3 and −1.4 kcal/mol, resp.). With NO_2, the large increases in ΔE(gas) are opposed by a large $\delta\Delta G$solv of −4.5 kcal/mol due to the hydrophilicity of this group. With —CF_3, conversely, $\delta\Delta G$solv is negligible (−0.2 kcal/mol), and both G4 and C16 contribute favorably to ΔE(gas). The favorable contribution of —CF_3 to C16 binding is due to its own stacking interactions with this base, possibly compensating for a lesser electron density around the CCl bond. Its contribution to G4 binding is due to

Table 3. Binding site of coagulation factor Xa.

		Tyrosine - halobenzyl			Formamide - halobenzyl		Ternary complex	
Complex B		$\delta\Delta E$ Solv	ΔE Gas	ΔE Gas - $\delta\Delta E$ Solv	ΔE Gas	ΔE Gas - $\delta\Delta$E Solv	ΔEGas	ΔE Gas - $\delta\Delta E$ Solv
Meta 3	NH_2	−5.38	−3.73	1.65	−0.96	4.42	−5.42	−0.04
	OH	−7.42	−0.22	7.2	−0.47	6.95	−0.46	6.96
	F	0	20.22 $\uparrow\alpha^+$	−0.22	0.41 $\downarrow\alpha^-$	0.41	0.22	0.22
	NO_2	−3.78	−0.85 $\uparrow\alpha^+$	2.93	1.08 $\downarrow\alpha^-$	4.86	0.55	4.33
Meta 5	NH_2	−5.37	−5.05	0.32	−1.2	4.17	−6.97	−1.6
	OH	−7.4	−0.23	7.17	−0.71	6.69	−0.73	6.67
	F	0	−0.27 $\uparrow\alpha^+$	−0.27	0.2 $\downarrow\alpha^-$	0.2	−0.03	−0.03
	NO_2	−3.78	−0.74 $\uparrow\alpha^+$	3.04	0.9 $\downarrow\alpha^-$	4.68	0.43	4.21
Ortho 2	NH_2	−3.77	−4.51	−0.74	−2.37	1.4	−6.57	−2.8
	OH	−2.82	−0.28	2.54	−0.56	2.26	−0.5	2.32
	F	−0.32	−1.03 $\uparrow\alpha^+$	−1.35	0.01 $\downarrow\alpha^-$	−1.35	−0.83	−2.18
	NO_2	−4.82	−2.55 $\uparrow\alpha^+$	2.27	0.14 $\downarrow\alpha^-$	4.96	−1.79	3.03
Ortho 6	NH_2	−3.84	−4.25	−0.41	−1.55	2.29	−6.19	−2.35
	OH	−2.67	−2.6	0.07	−0.4	2.27	−3.02	−0.35
	F	−0.33	−2.8 $\uparrow\alpha^+$	−2.47	0.22 $\downarrow\alpha^-$	0.55	−2.8	−2.47
	NO_2	−4.83	−0.88 $\uparrow\alpha^+$	3.95	1.63 $\downarrow\alpha^-$	6.46	1.32	6.15
Meta 3-5	2F	0.5	−0.49 $\uparrow\alpha^+$	−0.99	0.63 $\downarrow\alpha^-$	0.13	0.21	−0.29
Ortho 2-6	2F	−0.22	−0.48	−0.26	0.26	0.48	−0.08	0.14

Values (kcal/mol) of the desolvation and interaction energies and energy balances of substituted halobenzenes with respect to unsubstituted chlorobenzene.

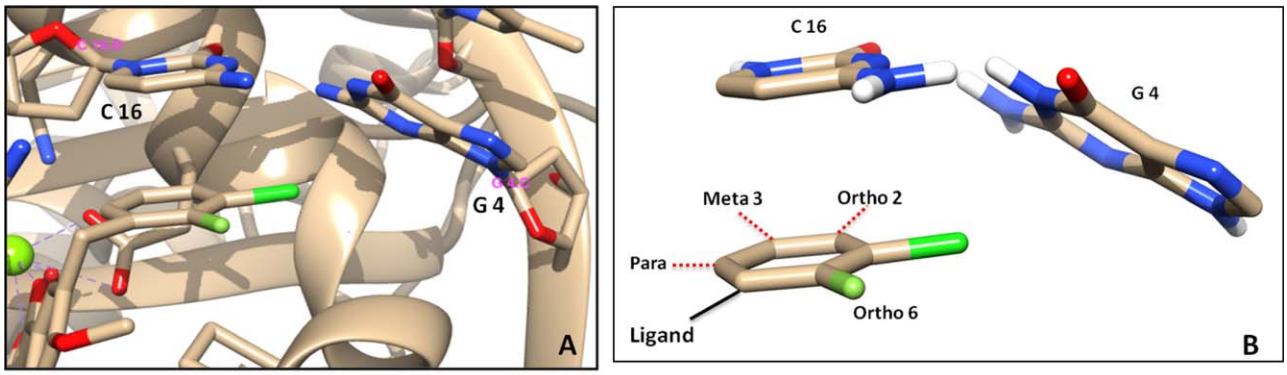

Figure 3. a) Representation of the binding site of viral integrase; and b) close-up on the interaction involving the halobenzene ring and notation of the substitution positions. [Color figure can be viewed in the online issue, which is available at wileyonlinelibrary.com.]

increasing electron depletion along the $\alpha+$ zone along the CCl bond.

The interaction energies in the ternary complexes are non-additive, as the value of ΔE(gas) differs from the sum of the ΔE(gas) values in the three binary complexes considered at the same geometry, namely halobenzene with G4 and with C16, and G4 with C16. Such interactions will be denoted as cooperative whenever ΔE(gas) is more stabilizing than such a sum, and by anticooperative whenener it is less stabilizing by it.

The most efficient electron-donating substitution is with a —$NHCH_3$ in ortho6, enabling the largest gain (−3.9 kcal/mol) found in the present study from monosubstitution. It is dominated by ΔE (gas), while $\delta\Delta$Gsolv opposes it by a small amount (1.2 kcal/mol). Such a substitution improves ΔE(gas) with G4 by −4.6 kcal/mol while it destabilizes it with C16 by 1.6 kcal/mol. There is a remarkable cooperativity effect on simultaneous binding of this compound to G4 and C16: thus ΔE(gas) amounts to −5.1 instead of −3.0 kcal/mol. In marked contrast, the simultaneous binding to G4 and C16 of chlorobenzene having a meta3 —$NHCH_3$ substituent is anticooperative: ΔE (gas) now amounts to −3.6 instead of −6.3 kcal/mol. Such unanticipated results imply that significant second-order polarization and charge-transfer effects can come into play in the stabilization/destabilization of the complexes of substituted halobenzenes. They have been analyzed[29] by both QC

Table 4. Binding site of viral integrase.

		C16 -halobenzyl			G4 - halobenzyl		Ternary complex	
Complex C		$\delta\Delta E$ Solv	δEGas	δE Gas – $\delta\Delta E$ Solv	δEGas	ΔE Gas – $\delta\Delta E$ Solv	ΔEGas	ΔE Gas - $\delta\Delta E$ Solv
Para	NH_2	−5.72	−1.86	3.86	−0.25	5.47	−0.8	4.92
	OH	−7.2	0.34	7.54	−1	6.2	−1.79	5.41
	$NHCH_3$	−4.15	−5.45	−1.3	−1.6	2.55	−4.22	−0.07
	NO_2	−3.52	−2.26	1.26	−1.52 $\uparrow\alpha^+$	2	−3.49	0.03
	F	0.08	0.39 $\downarrow\alpha^-$	0.31	−0.45 $\uparrow\alpha^+$	−0.53	0.12	0.04
	CF3	−0.21	−1.14	−0.93	−0.68 $\uparrow\alpha^+$	−0.47	−1.84	−1.63
Meta 3	NH_2	−5.05	−7.47 $\downarrow\alpha^-$	−2.42	2.95 $\uparrow\alpha^+$	8	−3.29	1.76
	OH	−7.09	0.72	7.81	1.65 $\uparrow\alpha^+$	8.74	2.37	9.46
	$NHCH_3$	−3.64	−5.71	−2.07	−0.56	3.08	−3.55	0.09
	NO_2	−3.46	−0.12	3.34	−0.22	3.24	−0.123	3.23
	F	0.32	0.45	0.13	0.99	0.67	1.68	1.36
	CF3	−0.19	−1.24	−1.05	1.13	1.32	0.02	0.21
Ortho 2	NH_2	−3.46	−3.7 $\downarrow\alpha^-$	−0.24	−0.75	2.71	−3.81	−0.35
	OH	−2.49	−3.39 $\downarrow\alpha^-$	−0.9	1.24 $\uparrow\alpha^+$	3.73	−2.08	0.41
	$NHCH_3$	−1.1	−3.19 $\downarrow\alpha^-$	−2.09	1.41 $\uparrow\alpha^+$	2.51	−1.79	−0.69
	NO_2	−4.49	−3.27	1.22	−4.2	0.29	−6.83	−2.34
	F	0.01	1.7	2.26	0.98	2.26	2.93	2.26
Ortho 6	NH_2	−3.52	−0.98	2.54	0.96	4.48	0.19	3.71
	OH	−2.34	0.21	2.55	0.55	2.89	0.87	3.21
	$NHCH_3$	−1.16	1.64	2.8	−4.62	−3.46	−5.09	−3.93
	NO_2	−4.49	−3.51	0.98	−3.15	1.34	−5.84	−1.35
	H	0.32	0.99	0.67	−0.97	−1.29	−0.51	−0.83
4F m3—p—o2—o6		1.08	2.46 $\downarrow\alpha^-$	1.38	−4.94 $\uparrow\alpha^+$	−6.02	−2.23	−3.31
NHCH3—o2 CF3—p		−1.64	−7.95	−6.31	−1.48	0.16	−6.87	−5.23
NHCH3—o2 2F—o6—p		−1.6	−7.23	−5.63	−0.95 $\uparrow\alpha^+$	0.65	−5.69	−4.09

Values (kcal/mol) of the desolvation and interaction energies and energy balances of substituted halobenzenes with respect to the unsubstituted chlorobenzene.

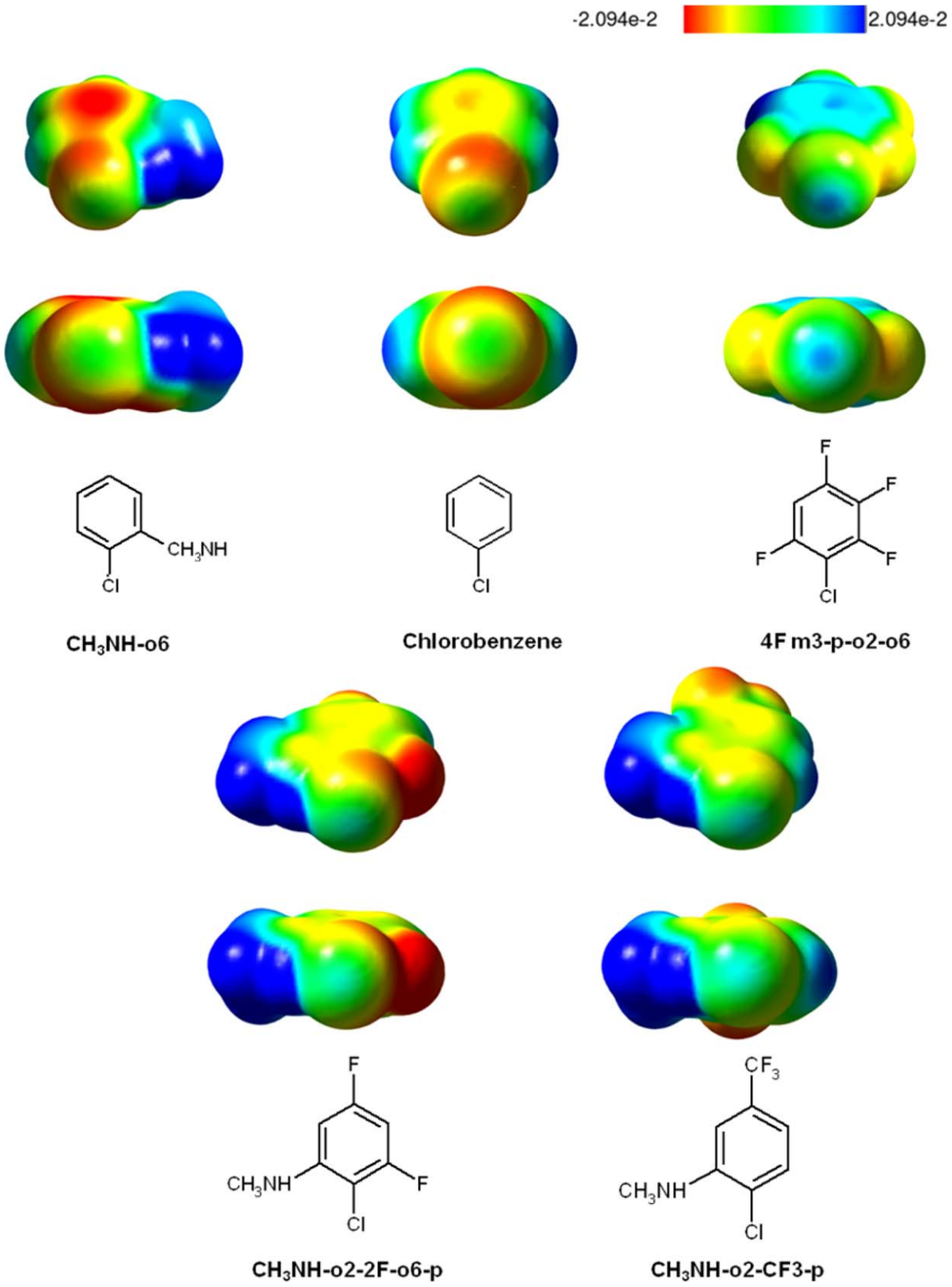

Figure 4. Mapping the MEP of four potent substituted chlorobenzene ligands of the HIV-1 integrase series, at the 0.0004 electrons Bohr^{-3} isodensity surface. The chlorine is facing the viewer in each plot. [Color figure can be viewed in the online issue, which is available at wileyonlinelibrary.com.]

Energy Decomposition Analyses[30] and the sum of interaction between fragments *Ab initio* (SIBFA) anisotropic polarizable molecular mechanics procedure.[31]

We then considered di- and up to tetrasubstitutions in an attempt to integrate together the most efficient monosubstitutions.

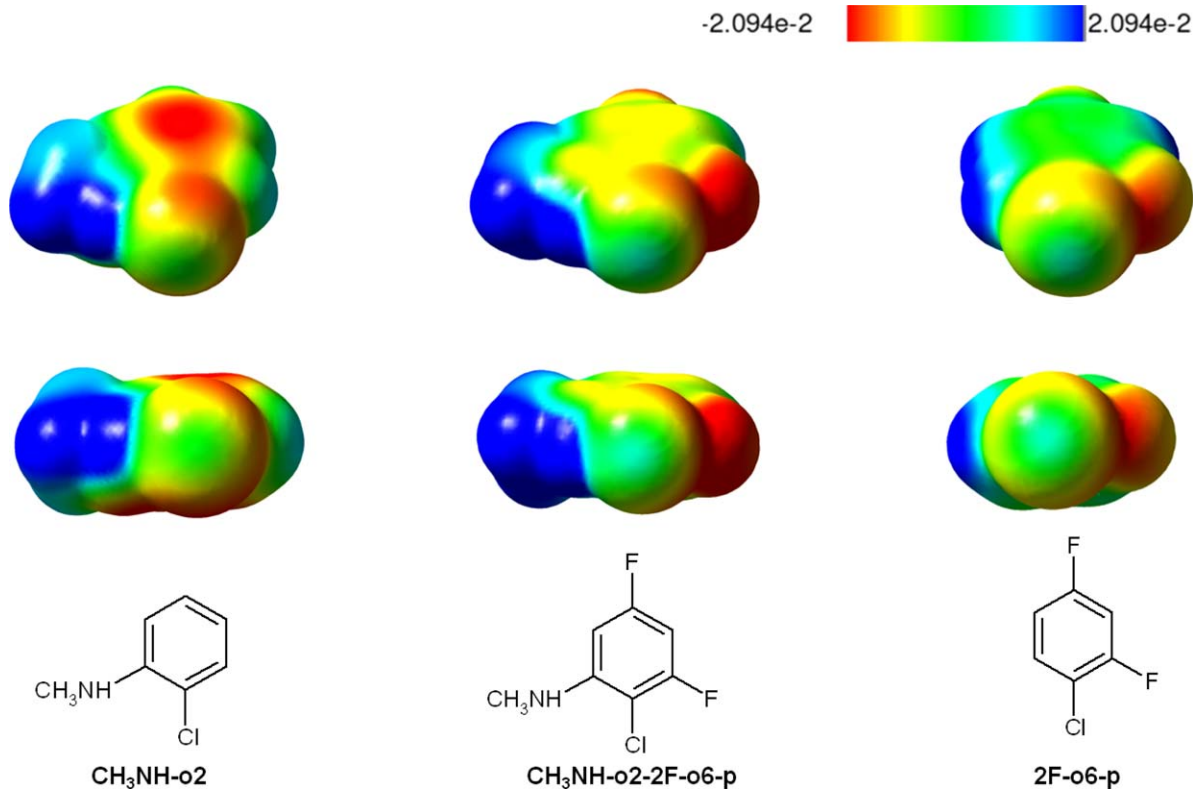

Figure 5. MEP mapping showing the "in-concert amplification" of the halobenzene ligand [CH_3NH—o2—2F—o6—p] of the HIV-1 integrase series, at the 0.0004 electrons $Bohr^{-3}$ isodensity surface. (left) electron-donor substituted halobenzene CH3NH—o2, (right) electron-attractor substituted halobenzene 2F—o6—p and (middle) halobenzene with both electron-donor and electron-attractor substituents CH_3NH—o2—2F—o6—p. The chlorine is facing the viewer in each plot. [Color figure can be viewed in the online issue, which is available at wileyonlinelibrary.com.]

With four F substituents, a $\delta\Delta E$ gain of −3.3 kcal/mol obtains, due to a significantly lessened $\delta\Delta G$solv of 1.1 kcal/mol and to an enhanced ΔE(gas) with G4 (−4.9 kcal/mol). The latter gain contrasts markedly with the summed effects of F-monosubstitutions, which is actually destabilizing (1.5 kcal/mol). This is another departure from nonadditivity, which reflects the impact of substitution on the electronic structure. It could also be accounted for by polarizable molecular mechanics on resorting to QC distributed multipoles and polarizabilities.[29] With the four F substituents, ΔE(gas) with C16 is destabilizing (2.5 kcal/mol). Such a destabilization is now close to the one resulting from the cumulated F monosubstitutions at ortho2, ortho6, meta3, and para (2.5 kcal/mol).

The largest $\delta\Delta E$ gains were due either: (a) to disubstitution: by, on the one hand, the electron-donating —$NHCH_3$ group in ortho2; and conversely, by the electron-withdrawing -CF_3 group in para (−5.2 kcal/mol); or (b) to trisubstitution: by —$NHCH_3$ in ortho2, and by disubstitution by —F in ortho-6 and in para (−4.1 kcal/mol).

In (a), a −3.6 kcal/mol energy gain due nonaddivity in polysubstitution is found for C16 binding (−8.0 as compared to −4.3 kcal/mol for the summed monosubstitutions) as well as a −2.2 kcal/mol energy gain for G4 binding (−1.5 as compared to +0.7 kcal/mol for the summed monosubstitutions). In the case of (b), such energy gains also occur by comparable amounts. Thus ΔE with C16 amounts to −7.2 kcal/mol, whereas the summed contributions of monosubstituting —$NHCH_3$ and the two F substituents amount to −3.8 kcal/mol ($\delta\Delta E$(gas)= −3.4 kcal/mol). ΔE with G4 amounts to −1.0 kcal/mol, whereas the summed contributions amount to 1.9 kcal/mol ($\delta\Delta E$(gas)= −2.9 kcal/mol).

We have mapped the electrostatic potentials of the four substituted compounds which afforded the largest energy gains and compared them to bare chlorobenzene (Fig. 4). The first is the CH3NH—o6 derivative, for which the NHCH3 electron-donor ortho to Cl increases the intensity of the red volume on the side of the CX bond opposite to it (leftmost figure on the first two rows). Conversely, for the second compound considered, the 4F (m3—p—o2—o6) derivative, the five electron-attracting fluorines are seen to abolish the presence of the red contours and to increase the positive potential around the whole molecule; this increase is particularly accented along the extension of the CX bond (rightmost figure on the first two rows). The largest $\delta\Delta E$ gains reported in Table 4 were due to the coexistence of an electron-donating group, namely CH3NH—, and of electron-attracting groups, as with the third and the fourth compounds, denoted as CH3NH—o2—2F—o6—p and CH3NH—o2—CF3—p. The first of these is represented in the two left figures of the last two rows and the second in the two right ones. It appears that for CH3NH—o2—2F—o6—p, the enhancements of both $\alpha-$ and $\alpha+$ zones can coexist. This is not the case, conversely, for CH3NH—o2—CF3—p, for which the electron attraction by CF3 has overcome the electron donation by NHCH3.

Table 5. ELF analyses results of the electronic population and its volume *V*(Cl) around the chlorine atoms in the most significant substituted derivatives.

V(Cl)	Chlorobenzene	CH3NH—O6	4F m3—p—o2—o6	CH3NH—O2—2F—o6—p	CH3NH-O2—CF3—p
Volume (Ua3)	231.69	233.34	216.32	224.92	229.91
Population (e-)	13.31	16.43	8.25	16.34	15.08

Populations are given in e-, and volumes in au^3

We have attempted to clarify to what an extent could the two facets of the "Janus-like" CX bond, $\alpha-$ and $\alpha+$, could be amplified jointly. Thus we have recast in Fig. 5 the MEP around derivative CH3NH—o2—2F—o6—p, in the central position, and compared it to those around derivatives CH3NH—o2 having a sole electron-donating group, and 2F—o6—p, having solely two electron-attracting groups. These two compounds are represented in the two left- and rightmost positions, respectively. For the central compound, with respect to the right-most compound, it appears that the intensity of the red zone on the side of the CX bond opposite to the NHCH3 substituent is greater than in its absence. It thus does not stem from the sole F substituent itself, despite its immediate proximity to this side of the $\alpha-$ zone, but from the electron-donating NHCH3 group. At the same time, the volume and intensity of the green contours of the $\alpha+$ zone prolonging the CX bond are clearly larger than with the left-most compound CH3NH—o2. Thus they do not stem from the sole effect of the imino and methyl hydrogens of this group, but are due to the electron-withdrawing nature of fluorine on the opposite site of the CX bond.

Such MEP features could be quantified in a more quantitative fashion on resorting to topological analyses, such as procedures developed by Gadre et al.[32] or the ELF.[24] Table 5 reports the results of ELF analyses of the volume of the electronic population as well as the electron population *V*(Cl) around chlorine in the most significant substituted derivatives and the electronic population. Supporting Information Figure 1 shows the volumes around the atoms and chemical bonds of chlorobenzene. Those around Cl and C4—Cl are marked with arrows. With respect to unsubstituted chlorobenzene, a comparison of these values (Table 5) shows an increase of the volume and of the population around Cl on substitution with the electron-donating group —$NHCH_3$ and a decrease on substitution with electron-withdrawing groups, such as four fluorine atoms. With rings having both electron-donating and electron withdrawing groups, the volumes have intermediate values while the electron populations have closer values to those found with the sole electron-donating substituent —$NHCH_3$. The analysis conducted on the ternary complexes and on the binary complexes shows similar variations in the volumes of the electronic population as with the uncomplexed rings.

Some recent papers indicate that in some complexes with halogenated compounds, either the binding affinities[33] or the orientation dependencies[34] could be dominated by the overlap-dependent contributions rather than electrostatics. This is not the case for the complexes investigated in this study. Recent energy-decomposition analyses[29] have indicated that the first-order Coulomb and the second-order polarization contributions, both of intrinsically electrostatic nature, are the predominant determinants in the modulation of affinities by chemical substitution.

Could, for the most interesting derivatives, substitution result in similar energy enhancements regardless of halogenation? To address this point, we did single-point calculations on replacing the Cl atom by an H one with a CH distance of 1.08 Å. The results are reported in Table 6. The energy results are given as differences with respect to the interaction energy of unsubstituted benzene taken as energy zero. The first column relates to bare chlorobenzene, and is followed by the results with four substituted compounds regrouped in pairs of rows. The first member of the pair has no chlorine (X=H) and the second member is chlorinated. It is observed that whatever the substituent, a clear energy gain, in the 2–6 kcal/mol range, obtains thanks to halogenation. It is to be noted that desolvation can significantly impact the balances. A more detailed analysis of the energy trends including nonadditivity and the role of correlation will be given in a separate paper. At this stage, considering the role of all these factors, the present findings imply that the differential impact of substitutions on halogenated versus nonhalogenated compounds could not simply be reduced to through-space effects as inferred by some recent studies.[35]

We have performed calculations with HF and other DFT functional, WB97x and M06-2X, on three representative complexes (the parent halobenzene ortho-6 F, as well as ortho-6 NHCH3 and CH3NH—o2 2F—o6—p) to evaluate if the trends

Table 6. Binding site of viral integrase. Comparison of the intermolecular interaction and desolvation energies of four substituted X-benzene rings (X=H versus X=Cl). The energy values are given with respect of the unsubstituted benzene taken as energy zero.

	X—benzene	NHCH3—o6		NHCH3—o2 2F—o2—p		NHCH3—o2 CF3—p		4F m—p—o2—o6	
Ternary Complex (kcal/mol)	X = Cl	X = H	X = Cl	X = H	X = Cl	X = H	X = Cl	X = H	X = Cl
ΔE Gas	−2.82	−7.01	−7.40	−5.01	−8.00	−6.06	−9.18	−3.84	−4.54
$\delta\Delta E$ Solv	0.20	−3.73	−1.28	−4.14	−1.72	−4.91	−1.76	−0.43	0.96
δE Gaz – $\delta\Delta E$ Solv	−3.02	−3.28	−6.12	−0.87	−6.28	−1.15	−7.42	−3.41	−5.50

Table 7. Values (kcal/mol) of the interaction energy ΔE and of the nonadditivity at HF and DFT levels.

	E Gas				Nonadditivity			
Complex C	HF	B97D	WB97x	M06-2X	HF	B97D	WB97x	M06-2X
Ortho 6 F	−17.93	−38.35	−33.31	−33.86	0.17	0.84	−0.14	−0.53
Ortho 6 $NHCH_3$	−24.10	−43.44	−41.10	−41.46	−1.29	−1.27	−2.05	−2.30
CH_3NH—o2 2F—o6—p	−18.43	−44.04	−40.28	−42.90	0.81	3.32	2.35	1.79

are preserved. The trends of both the interaction energies ΔE and nonadditivities are maintained (Table 7). Thus for a given level of DFT accuracy the exact form of the DFT functional should not be expected to alter the trends found in this study.

A very important implication of the above findings is that the effect of electron-donation or electron-withdrawal on halogen bonding interactions, should not focus on a single substituent at a time, and could be extended to di- and multiple substitutions, because for some conjugated rings these could act either cooperatively or anticooperatively, and imbalance one facet of the CX bond with respect to the other.

We provide as Supporting Information SI2 the coordinates of the ternary complexes of the most promising halobenzene derivatives with G4 and C16. The coordinates of the ternary complexes in the recognition sites of Ftase and coagulation FXa are available on request.

Impact of substitution on solvation

In several cases, desolvation emerged in this study as a key contributor to the energy balances. In this context, an unanticipated yet fully sensible, consequence of the introduction of substituent groups to halobenzenes is their ability to decrease in several cases the magnitude of ΔGsolv. This could be rationalized on the basis of the total molecular dipole moment μ to which they contribute. A near-linear correlation between μ and ΔGsolv is illustrated in Figure 6. In the majority of cases, the larger the dipole, the larger the magnitude of ΔGsolv. This correlation remains near-linear: thus a polar substituent can contribute to decrease the total molecular dipole if its own dipole tends to be antiparallel to that of another substituent, but it nevertheless contributes to ΔGsolv owing to its own local solvation.

Possible impact of entropy

Analyses of vibrational frequencies are only valid at a stationary point.[23] Such analyses would thus only be meaningful for the fully optimized ternary model systems, considering that the protein or DNA target fragments of complexes I–III were held fixed at their experimental positions. The total free energy ΔG and the total entropy ΔS along with the vibrational entropy $\Delta S_{vibrational}$ are represented in the Supporting Information SI3 and for the three halobenzenes (X=H, Cl and Br). The trends in ΔS_{Tot} are dominated by the vibrational entropy, whether progressing from the X=H series to the X=Br one, or, within a given series, on passing from electron-donating groups to electron-withdrawing ones of increasing size. Consistent with the results recently reported in Ref. [36], the ΔH gains are accompanied by concomitant ΔS losses. Nevertheless, in the present series, such relative losses are smaller than the ΔH gains and, in the present context, should not significantly impact the trends in the energy balances.

Conclusion and Perspectives

In this study we sought to leverage the dual nature of the CX bond in halobenzenes to enhance its binding affinity to model protein or DNA binding sites. We have attempted to go beyond the general endeavors in this domain limited to the $\alpha+$ region, on enhancing both electron-rich and electron-deficient sites of this bond.

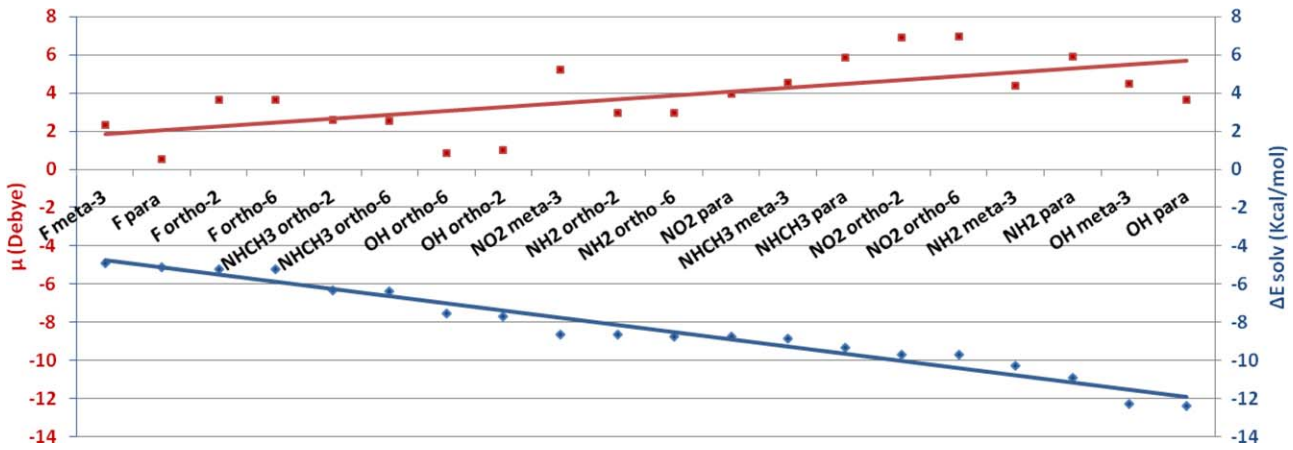

Figure 6. Correlation between the molecular dipoles and the Continuum solvation energies of the substituted halobenzenes. [Color figure can be viewed in the online issue, which is available at wileyonlinelibrary.com.]

The energy balances included solvation/desolvation. A synergy between desolvation and ΔE could be obtained in several cases. Thus the polyfluorinated substituent has a lower $\delta\Delta$Gsolv of 1.1 kcal/mol whence an enhanced ΔE of -3.3 instead of -2.2 kcal/mol. Two aspects of nonadditivity came into play. The first was observed on passing from binary to ternary complexes. The second was observed with multiple substitutions, affording in some cases significantly different ΔE enhancements than those resulting from the summed effects of monosubstitutions. Some notable examples were found in the binding site of HIV-1 integrase. Thus a disubstituted halobenzene with a CH_3NH group in ortho2 and a CF_3 group in para had a ΔE value of -6.9 kcal/mol, -3.2 kcal/mol more favorable than the sum of the monosubstitutions amounting to -3.6 kcal/mol.

This study could have a general scope even though it was limited to small oligoligated halobenzene complexes. It indicated that prior to large-scale MM, MD, or MC simulations on large protein-ligand complexes, a beneficial yet affordable prescreening with high-level QC could be undertaken. It has led to unanticipated results regarding nonadditivity: on the one hand, for poly- as compared to cumulated monosubstitutions; and conversely, owing to local polarization, charge-transfer and correlation, on passing from the binary to the ternary halobenzene complexes. Energy-decomposition analyses done on the HIV-1 recognition site showed that chemical substitutions impact predominantly the Coulomb and the polarization contributions.[29] These results and the present ones underline the role of both the dipole moments impacting the Coulomb contribution and the desolvation energy, and that of the polarizability impacting the polarization contrbution and nonadditivity. They provide a strong incentive for the applications of polarizable force fields embodying the desired physical effects thereby extending the realm of QC to very large systems.[31,37] The most promising derivatives from this study have been integrated in the structure of novel inhibitors of the HIV-1 integrase. MM and MD simulations of their complexes are presently underway and should be reported in due course.

Acknowledgments

The authors sincerely thank the Association Philippe Jabre for funding the PhD research of Krystel El Hage. The authors wish to thank the Grand Equipement National de Calcul Intensif (GENCI): Institut du Développement et des Ressources en Informatique Scientifique (IDRIS), Centre Informatique de l'Enseignement Supérieur (CINES), France, project No. x2009-075009), and the Centre de Ressources Informatiques de Haute Normandie (CRIHAN, Rouen, France), project 1998053. The authors also acknowledge the Research Council of Saint Joseph University of Beirut, Beirut, Lebanon (Project FS39), for financial support.

Keywords: sigma-hole · halobenzyl ring · electron-withdrawing substituents · electron-donating substituents · protein-ligand interactions · quantum chemistry · cooperativity · anticooperativity · rational drug design

How to cite this article: K. El Hage, J. P. Piquemal, Z. Hobaika, R. G. Maroun, N. Gresh . *J. Comput. Chem.* **2014**, DOI: 10.1002/jcc.23786

Additional supporting information may be found in the online version of this article.

[1] (a) T. Clark, M. Hennemann, J. S. Murray, P. Politzer, *J. Mol. Model.* **2007**, *13*, 291; (b) J. S. Murray, P. Lane, P. Politzer, *J. Mol. Model.* **2009**, *15*, 723; (c) P. Politzer, J. S. Murray, T. Clark, *Phys. Chem. Chem. Phys.* **2010**, *12*, 7748.

[2] (a) K. E. Riley, P. Hobza, *J. Chem. Theory Comput.* **2008**, *4*, 232; (b) K. E. Riley, J. S. Murray, P. Politzer, M. C. Concha, P. Hobza, *J. Chem. Theory Comput.* **2009**, *5*, 155; (c) J. Rezak, K. Riley, P. Hobza, *J. Chem. Theory Comput.* **2012**, *8*, 4285; (d) M. J. Palusiak, *Mol. Struct. Theochem.* **2010**, *945*, 89; (e) P. Romanielllo, F. Lelj, *J. Phys. Chem. A* **2002**, *106*, 9114; (f) Ibrahim, *J. Comput. Chem.* **2011**, *32*, 2564; (g) W. L. Jorgensen, P. Schyman, *J. Chem. Theory Comput.* **2012**, *8*, 3895; (h) M. Kolar, P. Hobza, *J. Chem. Theory Comput*. **2012**, *8*, 1325; (i) R. Wilcken, M. O. Zimmermann, A. Lange, A. C. Joerger, F. M. Boeckler, *J. Med. Chem.* **2013**, *56*, 1363 ; (j) J. S. Murray, P. Lane, P. Politzer, *J. Quantum Chem.* **2008**, *108*, 2770; (k) K. E. Riley, J. S. Murray, J. Fanfrlik, J. Rezac, R. J. Sola, M. C. Concha, F. M. Ramos, P. Politzer, *J. Mol. Model.* **2011**, *17*, 3309; (l) K. E. Riley, J. S. Murray, J. Fanfrlik, J. Rezac, R. J. Sola, M. C. Concha, F. M. Ramos, P. Politzer, *J. Mol. Model.* **2013**, *19*, 4651.

[3] L. A. Hardegger, B. Kuhn, B. Spinnler, L. Anselm, R. Ecabert, M. Stihle, B. Gsell, R. Thoma, J. Diez, J. Benz, J.-M. Plancher, G. Hartmann, D. W. Banner, W. Haap, F. Diederich, *Angew. Chem. Int. Ed.* **2011**, *50*, 314.

[4] Y. X. Lu, T. Shi, Y. Wang, H. Yang, X. Yan, X. Luo, H. Jiang, W. Zhu, *J. Med. Chem.* **2009**, *52*, 2854.

[5] R. Battistutta, *Cell. Mol. Life Sci.* **2009**, *66*, 1868.

[6] L. J. Liu, W. A. Baase, B. W. Matthews, *J. Mol. Biol.* **2009**, *385*, 595.

[7] H. Matter, M. Nazare, S. Gussregen, D. W. Will, H. Schreuder, A. Bauer, M. Urmann, K. Ritter, M. Wagner, V. Wehner, *Angew. Chem. Int. Ed.* **2009**, *48*, 2911.

[8] N. F. Valadares, L. B. Salum, I. Polikarpov, A. D. Andricopulo, R. C. Garratt, *J. Chem. Inf. Model.* **2009**, *49*, 2606.

[9] E. Parisini, P. Metrangolo, T. Pilati, G. Resnati, G. Terraneo, *Chem. Soc. Rev.* **2011**, *40*, 2267.

[10] (a) A. R. Voth, P. S. Ho, *Curr. Top. Med. Chem.* **2007**, *7*, 1336; (b) A. R. Voth, P. Khuu, K. Oishi, P. S. Ho, *Nat. Chem.* **2009**, *1*, 74.

[11] P. Auffinger, F. A. Hay, E. Westhof, P. S. Ho, *Proc. Natl. Acad. Sci.* **2004**, *101*, 16789.

[12] (a) J. P. M. Lommerse, A. J. Stone, R. Taylor, F. H. Allen, *J. Am. Chem. Soc.* **1996**, *118*, 3108; (b) K. E. Riley, P. Hobza, *Crystal Growth Des.* **2011**, *11*, 4272.

[13] (a) F. Dumitru, Y. M. Legrand, M. Barboiu, A. van der Lee, *Acta Crystallogr. B* **2013**, *69*, 43; (b) P. Politzer, J. S. Murray, T. Clark, *Phys. Chem. Chem. Phys.* **2013**, *15*, 11178.

[14] Y. Tong, N. H. Lin, L. Wang, L. Hasvold, W. Wang, N. Leonard, T. Li, Q. Li, J. Cohen, W. Z. Gu, H. Zhang, V. Stoll, J. Bauch, K. Marsh, S. H. Rosenberg, H. L. Sham, *Bioorg. Med. Chem. Lett.* **2003**, *13*, 1571.

[15] M. Nazare, D.W. Will, H. Matter, H. Schreuder, K. Ritter, M. Urmann, M. Essrich, A. Bauer, M. Wagner, J. Czech, M. Lorenz, V. Laux, V. Wehner, *J. Med. Chem.* **2005**, *48*, 4511.

[16] S. Hare, S. S. Gupta, E. Valkov, A. Engelman, P. Cherepanov, *Nature* **2010**, *464*, 232.

[17] S. Grimme, *J. Comput. Chem.* **2006**, *27*, 1787.

[18] (a) T. H. Dunning, *J. Chem. Phys.* **1989**, *90*, 1007; (b) D. Feller, *J. Comput. Chem.* **1996**, *17*, 1571.

[19] (a) H. B. Schlegel, *Theor. Chem. Acc.* **2003**, *66*, 333; (b) R. Fletcher, Practical Methods of Optimization; Wiley: New York, **1980**; (c) J. M. Bofill, *J. Comput. Chem.* **1994**, *15*, 1; (d) J. M. Bofill, M. Comajuan, *J. Comput. Chem.* **1995**, *16*, 1326; (e) J. Simons, P. Jorgensen, H. Taylor, J. Ozment, *J. Phys. Chem.* **1983**, *87*, 2745; (f) A. Banerjee, N. Adams, J. Simons, R. Shepard, *J. Phys. Chem.* **1985**, *89*, 52; (g) J. Baker, *J. Comput. Chem.* **1986**, *7*, 385; (h) J. Baker, *J. Comput. Chem.* **1987**, *8*, 563; (i) J. T. Golab, D. L. Yeager, P. Jorgensen, *Chem. Phys.* **1983**, *78*, 175.

[20] M. J. Frisch, G. W. Trucks, H. B. Schlegel, G. E. Scuseria, M. A. Robb, J. R. Cheeseman, G. Scalmani, V. Barone, B. Mennucci, G. A. Petersson, H. Nakatsuji, M. Caricato, X. Li, H. P. Hratchian, A. F. Izmaylov, J. Bloino, G. Zheng, J. L. Sonnenberg, M. Hada, M. Ehara, K. Toyota, R. Fukuda, J. Hasegawa, M. Ishida, T. Nakajima, Y. Honda, O. Kitao, H. Nakai, T. Vreven, J. A. Montgomery, Jr.; J. E. Peralta, F. Ogliaro, M. Bearpark, J. J. Heyd, E. Brothers, K. N. Kudin, V. N. Staroverov, R. Kobayashi, J. Normand, K. Raghavachari, A. Rendell, J. C. Burant, S. S. Iyengar, J. Tomasi, M. Cossi, N. Rega, N. J. Millam, M. Klene, J. E. Knox, J. B. Cross, V. Bakken, C. Adamo, J. Jaramillo, R. Gomperts, R. E. Stratmann, O. Yazyev, A. J. Austin, R. Cammi, C. Pomelli, J. W. Ochterski, R. L. Martin, K. Morokuma, V. G. Zakrzewski, G. A. Voth, P. Salvador, J. J. Dannenberg, S. Dapprich, A. D. Daniels, Ö. Farkas, J. B. Foresman, J. V. Ortiz, J. Cioslowski, D. J. Fox, Gaussian 09, Revision D.01; Gaussian, Inc.: Wallingford, CT, **2009**.
[21] (a) S. F. Boys, F. Bernardi, *Mol. Phys.* **1970**, *19*, 553; (b) S. Simon, M. Duran, J. J. Dannenberg, *J. Chem. Phys.* **1996**, *105*, 11024.
[22] (a) V. Barone, M. Cossi, *J. Phys. Chem. A.* **1998**, *102*, 1995; (b) M. Cossi, N. Rega, G. Scalmani, V. Barone, *J. Comput. Chem.* **2003**, *24*, 669.
[23] J. B. Foresman, M. J. Frisch, Exploring Chemistry with Electronic Structure Methods, 2nd ed.; Gaussian, Inc.: Pittsburgh, PA, **1996**.
[24] (a) A. D. Becke, K. E. Edgecombe, *J. Chem. Phys.* **1990**, *92*, 5397; (b) B. Silvi, A. Savin, *Nature* **1994**, *371*, 683; (c) J. P. Piquemal, J. Pilmé, O. Parisel, H. Gérard, I. Fourré, J. Bergès, C. Gourlaouen, A. De La Lande, M. C. Van Severen, B. Silvi, *Int. J. Quantum Chem.* **2008**, *108*, 1951.
[25] Y. Zhao, D. G. Truhlar, *Theor. Chem. Acc.* **2008**, *120*, 21.
[26] J. D. Chai, M. Head-Gordon, *J. Chem. Phys.* **2009**, *131*, 174105.
[27] (a) M. A. Ibrahim, *J. Comput. Chem.* **2011**, *32*, 2564; (b) S. Cabani, P. Gianni, V. Mollica, L. Lepori, *J. Solution Chem.* **1981**, *10*, 563.
[28] F. DeAnda, K. E. Hightower, R. T. Nolte, K. Hattori, T. Yoshinaga, T. Kawasuji, M. R. Underwood, *PLoS One* **2013**, *8*, e77448.
[29] K. El Hage, J.-P. Piquemal, Z. Hobaika, R. G. Maroun, N. Gresh, *J. Phys. Chem. A*, **2014**, *118*, 9772.
[30] (a) W. J. Stevens, W. Fink, *Chem. Phys. Lett.* **1987**, *139*, 15; (b) P. S. Bagus, K. Hermann, C.W. Bauschlicher, Jr., *J. Chem. Phys.* **1984**, *80*, 4378.
[31] N. Gresh, A. G. Cisneros, T. A. Darden, J.-P. Piquemal, *J. Chem. Theory Comput.* **2007**, *3*, 1960.
[32] (a) S. R. Gadre, C. H. Suresh, *J. Org. Chem.* **1997**, *62*, 2625; (b) C. H. Suresh, S. R. Gadre, *J. Am. Chem. Soc.* **1998**, *120*, 7049
[33] S. M. Huber, E. Jimenez-Izal, J. M. Ugalde, I. Infante, *Chem. Commun.* **2012**, *48*, 7708.
[34] A. J. Stone, *J. Am. Chem. Soc.* **2013**, *135*, 7005.
[35] (a) S. E. Wheeler, K. N. Houk, *J. Am. Chem. Soc.* **2008**, *130*, 10854; (b) S. E. Wheeler, K. N. Houk, *J. Chem. Theory Comput.* **2009**, *5*, 2301; (c) S. E. Wheeler, *J. Am. Chem. Soc.* **2011**, *133*, 10262.
[36] P. Politzer, J. S. Murray, *CrystEngComm* **2013**, *15*, 3145.
[37] K. El Hage, J.-P. Piquemal, Z. Hobaika, R. G. Maroun, N. Gresh, *J. Comput. Chem.* **2013**, *34*, 1125.

Received: 13 June 2014
Revised: 21 October 2014
Accepted: 27 October 2014
Published online on 00 Month 2014